PHYSICAL REVIEW B VOLUME 25, NUMBER 4 15 FEBRUARY 1982

Low-temperature microwave spectroscopy of Naβ-alumina

U. Strom
Naval Research Laboratory, Washington, D. C. 20375

M. von Schickfus and S. Hunklinger
Max-Planck-Institut für Festkörperforschung, D-7 Stuttgart 80, Federal Republic of Germany

(Received 24 August 1981)

Low-temperature microwave conductivity data for Naβ-alumina have been analyzed in terms of the standard tunneling model of disorder-induced two-level states. In addition, the microwave dielectric constant has been studied as a function of temperature between 0.3 and 15 K for Na, K, and $Na_{0.2}K_{0.8}\beta$-alumina. The limitations of the tunneling model in describing the conductivity and dielectric-constant data, particularly at higher temperatures (>5 K), are discussed. A direct relationship of the microwave conductivity to portions of the low-frequency loss in the 10^2-10^4-Hz region is established. It is shown that the low-frequency data require the existence of a temperature-independent conductivity term $\sigma\sim\omega^n$, where $n\cong 1$ for $T<1$ K. A brief discussion is given of the possible origin of tunneling modes in β-alumina.

I. INTRODUCTION

The fast-ion conductor Naβ-alumina has been studied by numerous optical, structural, and resonance experiments. Among the early studies were measurements of the far-infrared optical reflectivity,[1] which established that the local motion of the Na cations within the conduction planes of Naβ-alumina is essentially uncoupled from the rigid spinel-like blocks which separate the conduction planes. More refined infrared[2,3] and Raman measurements[2,4] concluded that the optical activity is not only due to single-ion motion but may involve pairs or larger groups of cations. Such a conclusion was supported by calculations of ionic transport in β-alumina which considered pairs of cations at interstitial sites.[5] These calculations were based in part on proposals by Whittingham and Huggins[6] and x-ray structural studies by Peters *et al.*[7]

The proposed occupation of interstitial sites by Na ions, as well as the presence of additional charge-compensating oxygen ions, introduces a considerable degree of configurational disorder within the conduction planes. This disorder may lead to "excess" optical activity, particularly at frequencies below the characteristic lattice modes of the solid. The possibility that disorder-induced low-frequency excitations may be important in β-alumina was first suggested in an attempt to explain the observation of an excess ionic conductivity measured at microwave frequencies.[8] It was proposed that there exist ions or groups of ions which can exist in energetically nearly equivalent configurations which are separated by a potential barrier. At sufficiently high temperature, thermally activated transitions over these barriers become possible which lead to additional contributions to the dielectric loss. At low temperatures, thermal excitations will be less likely, but quantum-mechanical tunneling between nearly equivalent configurations may become significant.

The existence of low-energy excitations was further confirmed by low-temperature thermal measurements. Analogous to similar measurements in glasses, the low-temperature specific heat of Naβ-alumina exhibits a contribution which is nearly linear in temperature.[9,10] The magnitude of the linear term decreases with increasing cation radius, as in the case of Na^+ being replaced by K^+ or Rb^+. In addition, thermal-conductivity measurements revealed an anomalous quadratic temperature dependence at low temperatures.[11] Both observations were related to the presence of energetically low-lying structural modes. Such modes can be modeled either as low-energy harmonic-phonon modes or as highly anharmonic tunneling systems. The definitive identification of these modes as two-level tunneling systems (TLS) was made possible by the observation of microwave

power saturation of the low-temperature microwave ionic conductivity.[12] Although the results agreed qualitatively with model predictions, no detailed theoretical analysis was presented. Such an analysis is important from the standpoint of understanding the microscopic details of the low-temperature ionic response. It also serves as a test case for the suitability of present theory for describing the low-temperature behavior of a wide range of disordered materials.

In this paper we present an extensive analysis of the low-temperature microwave conductivity data for Naβ-alumina in terms of a two-level tunneling model. Further, the interpretation is extended to additional measurements of the low-temperature dielectric constant of Kβ-alumina and the mixed-cation material $Na_{0.2}K_{0.8}\beta$-alumina.The analysis is applied to the low-temperature dielectric loss data of Anthony and Anderson for Naβ-alumina for the 10^2 to 10^4 Hz spectral region.[13] Finally, measurement of the relaxation times T_1, T_2 will be discussed briefly. A more direct measurement of relaxation times with microwave electric-field-echo experiments[14] at temperatures below 0.1 K will be described in a subsequent paper.

The present paper is structured as follows. The discussion of the experimental procedure in Sec. II is followed by the presentation and discussion of the experimental results in Sec. III. The conclusion in Sec. IV contains a brief summary of the pertinent findings of this study.

II. EXPERIMENTAL PROCEDURE

The samples consisted of small parallellepipeds ($1\times1\times24$ mm^3) cut with a diamond string saw from larger single crystals of melt-grown Naβ-alumina (obtained from Union Carbide Corp.). Samples cut from the same single-crystal material were studied previously with dc contact-free conductivity[15] and Raman-ir techniques.[2] The sample rods were placed with their long axes parallel to the maximum electric field of an X-band TM_{010}-mode cylindrical transmission cavity. Only a relatively small fraction of the cavity volume V was filled by the sample volume v, with typical values of $v/V\approx0.02$. For such a case the distribution of the electric fields in the cavity remains sufficiently undisturbed so that simple perturbation expressions[16] for the change in resonance frequency f_0 and cavity quality factor Q_0 can be related to the real and imaginary parts of the complex dielectric constant $\epsilon_c=\epsilon+i\epsilon''$. Generally the results are expressed in terms of the conductivity σ. In mks units $\sigma(\Omega^{-1}\,\mathrm{m}^{-1})$ is related to ϵ'' by $\sigma=\omega\epsilon_0\epsilon''$ where

$$\epsilon_0\cong(1/36\pi)\times10^{-9}\ \Omega^{-1}\,\mathrm{m}^{-1}\,\mathrm{sec}\ .$$

Both a copper cavity ($Q_0\sim4000$) and a superconducting Nb cavity ($Q_0>100\,000$ for $T<8$ K) were used. The cavities were placed in good thermal contact with a cold ^{3}He reservoir. The temperature was lowered by means of pumping on the ^{4}He and ^{3}He reservoirs and raised by means of a heater attached to the cavity.

The microwave spectrometer included an X-band (8—12 GHz) sweep oscillator which provided the input power for the microwave cavity. The cavity output signal was mixed with the output of a second X-band sweep oscillator which was tuned 30 MHz off the cavity frequency. The mixed signal was detected and amplified at 30 MHz. One sweep oscillator was locked to the microwave cavity frequency by means of a frequency stabilizer. For a typical loaded cavity Q of 10 000 the system was sufficiently sensitive to detect changes in the cavity frequency of one part in 10^7. Further details of the experimental technique have been described elsewhere.[17]

III. RESULTS AND DISCUSSION

A. Microwave conductivity data

Measurements of the microwave conductivity are shown in Fig. 1. The microwave ionic conductivity σ (in Ω^{-1} cm^{-1}) is plotted versus temperature for the case of the microwave electric field $\vec{F}$ perpendicular to the $\hat{c}$ axis of the β-alumina crystal, i.e., parallel to the conducting planes. Reports of microwave measurements for $\vec{F}||\hat{c}$ show that the microwave absorption is orders of magnitude smaller perpendicular to the conducting planes.[18] The measured conductivity at 11.5 GHz exhibits the following essential features: (1) For all temperatures, $\sigma(11.5\ \mathrm{GHz})>\sigma(\mathrm{dc})$. (2) The high-temperature (>50 K) conductivity follows a power-law behavior $\sigma\sim T^{\beta}$ where $\beta\sim2.1$. (3) There is an inflection in the conductivity curve near 25 K. (4) The conductivity increases with decreasing temperature below 5 K. (5) For $T\lesssim5$ K, the conductivity is dependent on the magnitude of the microwave power (see Fig. 1 of Ref. 12).

The listed features are consistent with a model in which the disorder in the conduction planes allows for local ionic motion which is dominated by

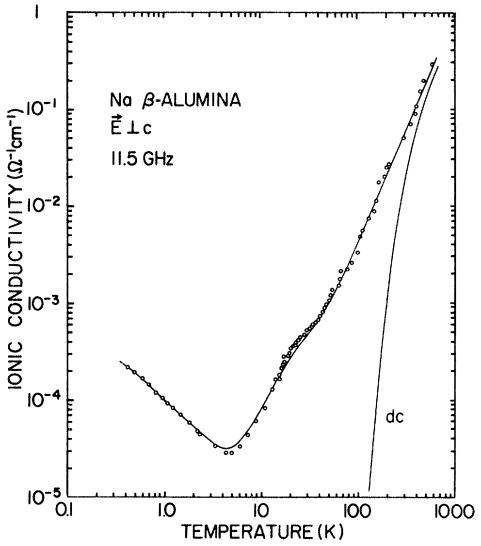

FIG. 1. Microwave ionic conductivity of Naβ-alumina [$(Na_2O)_{1.25}\cdot 11Al_2O_3$]. Circles: data; solid line: theoretical fit with Eq. (1); dc ionic conductivity from Ref. 6.

thermally activated processes at high temperatures and quantum-mechanical tunneling at low temperatures. Optical coupling to these modes leads to microwave absorption which is in excess of that expected for purely long-range diffusive transport. It will be shown that the experimental results at 11.5 GHz can be interpreted in terms of the following relation:

$$\sigma(T,11.5\ \text{GHz})=\sigma_S(T)+BT^{\beta}\,, \tag{1}$$

where $\sigma_S(T)$ is the conductivity derived from a two-level system tunneling-mode formalism. The second term in Eq. (1) is a phenomenological expression for the experimental results above 50 K up to the highest temperatures ($\sim$700 K). Although σ_S and BT^{β} may be intimately related, no satisfactory unified treatment exists at present. We will therefore assume that the second term in Eq. (1) holds down to the lowest temperatures studied with constant values for B and β. This assumption allows us to separate the experimental data into a contribution corresponding to BT^{β} and a remaining term $\sigma_S(T)$ which will provide a test for the tunneling model.

B. Tunneling model and fit to microwave conductivity data

The "standard" tunneling model as applied to the low-temperature properties of disordered solids has been discussed in detail by Jäckle,[19] Hunklinger and Arnold,[20] Graebner and Golding,[21] Black and Halperin,[22] and Black.[23] In addition, dielectric loss due to TLS is discussed by Anthony and Anderson.[13] We will briefly outline the model here. Details can be found in the above references.

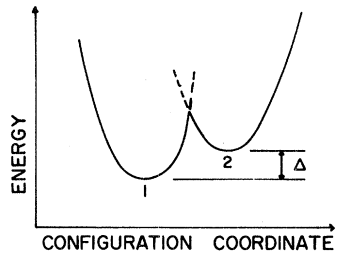

FIG. 2. Configurational diagram of tunneling mode.

The configuration coordinate diagram which describes a given tunneling mode is shown in Fig. 2. The barrier height and configurational coordinate spacing are of such magnitude that an atom (or group of atoms) corresponding to position 1 has a finite probability of occupying configuration 2 by tunneling through the separating barrier. In fact, the system shuttles back from configuration 1 to 2 with frequency Δ_0/h, where

$$\Delta_0=\hbar\Omega e^{-\lambda} \tag{2}$$

is the overlap energy, Ω is the zero-point angular-vibration frequency of the particle in one well, λ is a tunneling parameter, and h is Planck's constant. If the configurational coordinate is described by a distance d between wells with barrier height V, then $\lambda=d(2mV/\hbar^2)^{1/2}$, where m is the mass of the tunneling system. The unperturbed Hamiltonian in the basis of states $|1\rangle$ and $|2\rangle$ is

$$H_0'=\frac{1}{2}\begin{bmatrix}\Delta & \Delta_0\\ \Delta_0 & -\Delta\end{bmatrix}, \tag{3}$$

where Δ is the asymmetry energy as shown in Fig. 2. The states $|1\rangle$ and $|2\rangle$ are not eigenstates of the system. We define the states $|a\rangle$, $|b\rangle$ as eigenstates which diagonalize H_0' to yield

$$H_0=\frac{1}{2}\begin{bmatrix}E & 0\\ 0 & -E\end{bmatrix}, \tag{4}$$

where $E=(\Delta^2+\Delta_0^2)^{1/2}$. An applied oscillating tric field $\vec{F}$ will couple to the dipole moment $\vec{p}$ of a given tunneling mode. In the basis $|1\rangle, |2\rangle$ the interaction is

$$H_1'=-\vec{p}\cdot\vec{F}\begin{bmatrix}1 & 0\\ 0 & -1\end{bmatrix}, \tag{5}$$

or in the basis $|a\rangle, |b\rangle$

$$H_1 = -\frac{\vec{p}\cdot\vec{F}}{E}\begin{bmatrix}\Delta & \Delta_0\\ \Delta_0 & -\Delta\end{bmatrix}, \tag{6}$$

such that the total Hamiltonian is $H = H_0 + H_1$. The interaction term H_1 may induce resonant transitions between $|a\rangle$ and $|b\rangle$ through the off-diagonal elements of Eq. (6), or may perturb the level spacing E through the diagonal elements of H_1. The product $\vec{p}\cdot\vec{F}$ generally must be averaged over all directions. We will assume that $\langle\vec{p}\cdot\vec{F}\rangle = pF$, where p represents an average dipole moment of TLS in the conduction plane of β alumina.

The Hamiltonian H is equivalent to the case for a spin-$\frac{1}{2}$ system in a magnetic field. The dynamics of the spins are described by the Bloch equations which can be solved to yield the following expressions for the resonant absorption $\alpha_{\rm res}$ of radiation with angular frequency ω by a system of tunneling modes:

$$\alpha_{\rm res} = \frac{4\pi^2\omega\bar{P}p^2}{c\sqrt{\epsilon}}\left[1+\frac{J}{J_c}\right]^{-1/2}\tanh\hbar\omega/2kT\ , \tag{7}$$

where $\bar{P}$ is the density of states of tunneling modes which is assumed to be a constant for the energies considered here, and J is the microwave power. The critical-power level J_c is given by

$$J_c = \frac{\hbar^2 c\sqrt{\epsilon}}{8\pi p^2 T_1 T_2}\ , \tag{8}$$

where T_1 and T_2 are the relaxation times of the TLS due to their coupling to phonons and to other tunneling modes, respectively. For low power levels ($J < 0.01$ mW/cm^2 at 11.5 GHz) the condition $J << J_c$ is fulfilled and the low-temperature absorption accurately reflects the predicted $\tanh\hbar\omega/2kT$ dependence of Eq. (7).[12] [Note, that absorption α and conductivity σ are used interchangeably since they are directly related by $\sqrt{\epsilon}\alpha(\text{cm}^{-1}) = 120\pi\sigma(\Omega^{-1}\text{cm}^{-1})$]. The magnitude of the absorption below ~ 3 K yields the product $\bar{P}p^2$. For $\omega = 2\pi(11.5\times10^9)$ sec^{-1} in Eq. (7) and $J << J_c$, we find $\bar{P}p^2 = 1.7\times10^{-3}$.

Above $T\sim 5$ K in Naβ-alumina the resonant excitation of TLS no longer dominates and we need to consider the contribution of relaxation effects, i.e., the contribution of the diagonal elements of the interaction Hamiltonian H_1. This absorption has its origin in the modulation of the energy spacing E of the TLS by the microwave electric field and their subsequent relaxation via coupling to the phonon bath. With the assumption of a direct one-phonon process the TLS relaxation time is given by

$$T_1^{-1} = A\Delta_0^2 E\coth E/2kT\ . \tag{9}$$

The coefficient A is defined as

$$A = \left[\frac{\gamma_l^2}{v_l^5}+2\frac{\gamma_t^2}{v_t^5}\right]\frac{1}{2\pi\rho\hbar^4}\ , \tag{10}$$

where ρ is the mass density, γ_l,γ_t are the longitudinal and transverse deformation potentials, and v_l, v_t are the acoustic-phonon velocities. The minimum relaxation time $T_{\rm min}$ is given by Eq. (9) for $\Delta_0 = E$, i.e., for the case of a symmetric double well, as

$$T_{\rm min}^{-1} = AE^3\coth E/2kT\ , \tag{11}$$

so that

$$T_1^{-1} = T_{\rm min}^{-1}\left[\frac{\Delta_0}{E}\right]^2 .$$

The absorption due to relaxation processes is given by

$$\alpha_{\rm rel} = \frac{8\pi p^2\omega^2}{c\sqrt{\epsilon}} \times\int_0^\infty dE\,\frac{\partial f}{\partial E}\int_{T_{\rm min}}^\infty \frac{T_1}{1+\omega^2T_1^2}\frac{\Delta^2}{E^2}P(E,T_1)dT_1\ . \tag{12}$$

With $f = (\exp E/kT+1)^{-1}$ and

$$P(E,T_1) = -\frac{\bar{P}}{2T_1}(1-T_{\rm min}/T_1)^{-1/2}\ ,$$

Eq. (12) can be rewritten as

$$\alpha_{\rm rel} = +\frac{2\pi\bar{P}p^2}{c\sqrt{\epsilon}}\int_0^\infty dE\,\text{sech}^2E/2kT \times\int_{T_{\rm min}}^\infty dT_1\,\frac{(1-T_{\rm min}/T_1)^{1/2}}{1+\omega^2T_1^2}\ . \tag{13}$$

Two limiting cases of Eq. (13) are of interest: for $\omega T_{\rm min} << 1$,

$$\alpha_{\rm rel} = \frac{2\pi^2}{c\sqrt{\epsilon}}\bar{P}p^2\omega\ , \tag{14}$$

and for $\omega T_{\rm min} >> 1$,

$$\alpha_{\rm rel} = \frac{\pi^5\bar{P}p^2}{3c\sqrt{\epsilon}}Ak^3T^3\ , \tag{15}$$

where $\omega T_{\rm min} << 1$ represents the "high"-

temperature regime and $\omega T_{\min} >> 1$ describes the "low"-temperature behavior of $\alpha_{\rm rel}$. The data in Fig. 1 between $T \sim 5$ and 50 K are a superposition of $\sigma_S(T) = \sigma_{\rm res} + \sigma_{\rm rel}$ and BT^{β} [as expressed in Eq. (1)]. In order to fit only $\sigma_{\rm rel}$ we separate these three contributions assuming the form for $\sigma_{\rm res}$ (or equivalently $\alpha_{\rm res}$) in Eq. (7) and a low-temperature extrapolation of the BT^{β} conductivity contribution. The resulting experimental points for $\sigma_{\rm rel}$ are shown in Fig. 3. The fit to the data using $\bar{P}p^2 = 4.3 \times 10^{-3}$ and $A = 2.5 \times 10^6$ sec^{-1} K^{-3} is shown by the solid curve in Fig. 3.

Note that A is proportional to the slope of the low-T conductivity [see Eq. (15)], whereas the magnitude of $\sigma_{\rm rel}$ at high temperatures is proportional only to $\bar{P}p^2\omega$ [see Eq. (14)]. As seen in Fig. 3 the smaller value of $\bar{P}p^2 = 1.7 \times 10^{-3}$ does not lead to a satisfactory fit to the data. There is some uncertainty in the magnitude of A. This is due in part to the somewhat questionable extension of the BT^{β} to the lowest temperatures. Nevertheless, we do not expect that the possible values for A fall significantly outside the range from 1×10^6 to 5×10^6 sec^{-1} K^{-3}. However, even with the stated set of optimum parameters, there are some deviations between theory and experiment near $T \sim 5$ and 25 K. This is more evident in Fig. 1 where the solid line represents the total fit of $\sigma = \sigma_{\rm rel} + \sigma_{\rm res} + BT^{\beta}$ to the data using $(\bar{P}p^2)_{\rm rel} \cong 2.7(\bar{P}p^2)_{\rm res}$, where $(\bar{P}p^2)_{\rm res} = 1.7 \times 10^{-3}$ and $A = 2.5 \times 10^6$ sec^{-1} K^{-3}. We postulate that these deviations may be due to competing stronger temperature-dependent relaxation effects, such as the one-phonon Raman relaxation which is discussed in the Appendix.

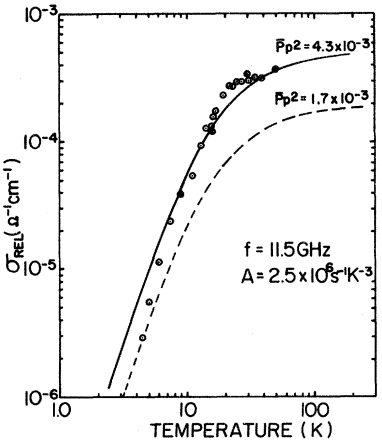

FIG. 3. Relaxation contribution $\sigma_{\rm rel}$ of tunneling modes to microwave ionic conductivity in Naβ-alumina. Data obtained from Fig. 1 after separation of resonant ($\sigma_{\rm res} \sim T^{-1}$) and high-temperature BT^{β} conductivity. Theoretical fits shown for different prefactors $\bar{P}p^2$ and $A = 2.5 \times 10^6$ cm^{-1} K^{-3}.

These results suggest that a *single* value of $\bar{P}p^2$ does *not* satisfactorily describe both resonant and relaxation contributions to the low-temperature microwave absorption. This is contrary to the tunneling model as initially proposed and outlined here. We have attempted to correct this difficulty by introducing off-diagonal components in the interaction Hamiltonian H_1' [Eq. (5)] as follows:

$$\tilde{H}_1' = - \begin{bmatrix} \vec{P}_1 & \vec{P}_2 \\ \vec{P}_2 & -\vec{P}_1 \end{bmatrix} \cdot \vec{F} , \tag{16}$$

so that $\tilde{H}_1 = H_1$ for $\vec{p}_2 = 0$. The resulting cumbersome calculation of the absorption, however, does not yield the necessary required result of $(\bar{P}p^2)_{\rm rel} \sim 2.7(\bar{P}p^2)_{\rm res}$ for any values of $\vec{p}_1$, $\vec{p}_2$. An alternative approach to remove this difficulty may be the consideration of an energy-dependent density of states $P(E)$. This has been attempted for β-alumina by Anthony and Anderson.[13] Specifically, they assumed[13] that

$$P(E) \sim P_m(E/kT_n)^{0.2} + P_n(E/kT_n)^3 ,$$

where $T_n \sim 1$ K in order to fit low-temperature susceptibility in the $10^2 - 10^4$ Hz region. Although they can fit their data with one value for $\bar{P}p^2$ they find consistent agreement between susceptibility and thermal conductivity only for $(\bar{P}p^2)_{\rm rel} \cong 2.9(\bar{P}p^2)_{\rm res}$. Unequal relaxation and resonant contributions are not unique to β-alumina. It has been shown[17] that the dielectric loss in glasses (SiO_2,As_2S_3, etc.) exhibits the condition $(\bar{P}p^2)_{\rm rel} > (\bar{P}p^2)_{\rm res}$. Finally, Golding *et al.*[24] have found that low-temperature acoustic experiments in a metallic glass could be understood in terms of the coupling to TLS to conduction electrons. Relaxation and resonant contributions could be defined as for the case of glasses, but in order to fit experiment an *additional* parameter had to be introduced which determined the relative sizes of relaxation and resonant contributions.

It can therefore be concluded that the two-level tunneling model as outlined in Eqs. (2)–(13) does not provide a unique description of the dielectric properties of disordered solids in terms of a single value for $\bar{P}p^2$. The difficulty lies mainly in the higher-temperature relaxation regime where the interaction with or modulation due to phonons may alter the simple TLS-model assumptions. Addi-

tional relaxation processes, such as the one-phonon Raman process discussed in the Appendix, should be considered in an attempt to remove these difficulties of the standard tunneling model.

C. Saturation of microwave conductivity

The microwave absorption of Naβ-alumina below 5 K is dependent on the intensity of the microwave radiation. This is expected for two-level systems which are excited with a power level equal to or greater than a critical power level J_c. The magnitude of J_c depends on the relaxation times T_1 and T_2. According to Eq. (7) the conductivity at a power level J is related to the conductivity for $J \rightarrow 0$ by

$$\sigma(J)=\sigma(0)(1+J/J_c)^{-1/2} .$$

The previously published saturation data[12] for Naβ-alumina have been replotted in Fig. 4 for temperatures of 0.5, 0.73, and 1.0 K. The solid lines are obtained from the above equation. The critical power levels for each of the temperatures are also indicated in Fig. 4. Theory and experiment are seen to agree for $J \sim J_c$. Significant deviations occur for $J >> J_c$. The cause of these deviations may be a microwave-radiation-induced phonon

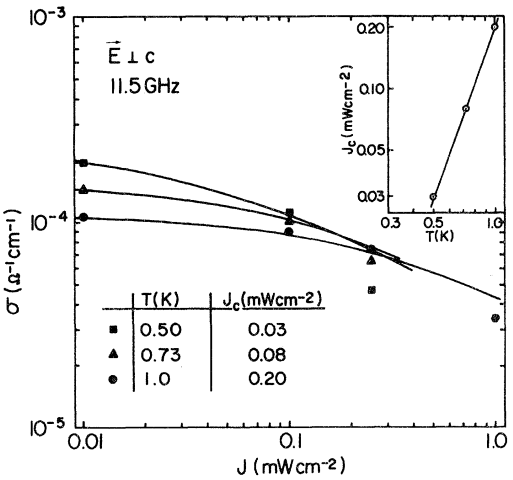

FIG. 4. Power saturation of microwave ionic conductivity in Naβ-alumina. Symbols: data from Ref. 12. Curves: predicted saturation dependence of tunneling model. Inset: temperature dependence of critical power density.

bottleneck; i.e., a large density of phonons is injected which has energies comparable to the energy spacing of resonantly excited TLS. These phonons can re-excite TLS and effectively increase the TLS lifetime and thus decrease J_c.

The temperature dependence of J_c is shown in the inset of Fig. 4. For the limited data available we infer that $J_c \sim T^{2.7}$ for T between 0.5 and 1.0 K. For Suprasil I at 10 GHz over the same temperature range it is found that[17] $J_c \sim T^{3.8}$. The observed temperature dependences of Naβ-alumina and Suprasil I glass are difficult to understand on the basis of Eq. (8) and the expected temperature dependences for T_1 [Eq. (9)] and T_2.[20] Low-temperature pulsed microwave electric-field-echo experiments in Naβ-alumina[14] and Suprasil I (Ref. 25) provide evidence for the importance of spectral diffusion,[22] i.e., a mechanism for the loss of phase memory of a system of TLS pseudospins. It has been found that at temperatures below 1 K spectral diffusion is the dominant mechanism responsible for echo decay. Black and Halperin[22] have made predictions concerning the expected temperature dependence of effective T_1, T_2 for a process in which TLS interact by means of the thermal-phonon bath. These predictions can be shown to fail for Naβ-alumina in that considerably weaker temperature dependences are actually observed for the echo decay times.[14] The physical origin for this different temperature dependence can be found in the much weaker coupling of TLS to phonons in Naβ-alumina compared to typical glasses. We suggest that spectral diffusion may be important in the saturation measurements at 10 GHz, and further that the different temperature dependences observed for J_c in Naβ-alumina and SiO_2, may be related to fundamentally different mechanisms for spectral diffusion in these two representative solids.

D. Low-temperature dielectric constant

The observed low-temperature variation of the dielectric constant is shown in Fig. 5. The contrasting temperature dependence for the resonant and relaxation contributions leads to a characteristic minimum. As seen in Fig. 5, the minimum is sensitively dependent on cation type. The data in Fig. 5 were obtained using a single sample, starting with Naβ-alumina and subsequently substituting K for Na. (The substitution technique was as follows[2]: to obtain $Na_{0.25}K_{0.75}\beta$-alumina, the crystal was immersed in a solution of equal parts of mol-

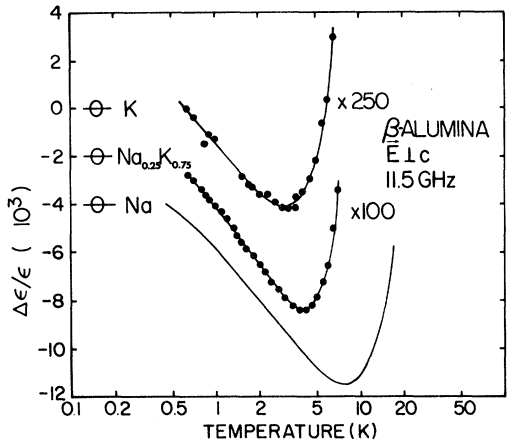

FIG. 5. Temperature dependence of variation of dielectric constant $\Delta\epsilon$ for $Na_xK_{1-x}\beta$-alumina at 11.5 GHz. Curves are offset vertically for clarity.

ten $NaNo_3$ and KNO_3 at 350°C for a period of 72 h; for Kβ-alumina a solution of KNO_3 at 350°C was used.)

Application of the Kramers-Kronig relation to Eqs. (7) and (12) leads to the following expression for $\Delta\epsilon_{\rm rel}$, where $\Delta\epsilon_{\rm rel}(T)\equiv\epsilon_{\rm rel}(T)-\epsilon_{\rm rel}(T_0)$ and T_0 is an arbitrary reference temperature:

$$\Delta\epsilon_{\rm rel}=\frac{2\pi\bar{P}p^2}{kT}\int_0^\infty dE\,\mathrm{sech}^2\frac{E}{2kT}\times\int_{T_{\rm min}}^\infty\frac{dT_1}{T_1}\times\frac{(1-T_{\rm min}/T_1)^{1/2}}{1+\omega^2T_1^2}\,. \tag{17}$$

The change in the dielectric constant due to the resonant interaction with TLS

$$\Delta\epsilon_{\rm res}\equiv\epsilon_{\rm res}(T)-\epsilon_{\rm res}(T_0)\,,$$

is given by

$$\Delta\epsilon_{\rm res}=-8\pi\bar{P}p^2\ln\frac{T}{T_0}\,. \tag{18}$$

The total change in the dielectric constant $\Delta\epsilon_{\rm total}=\Delta\epsilon_{\rm rel}+\Delta\epsilon_{\rm res}$ will have a minimum at a temperature T_m which is determined primarily by the parameter $T_{\rm min}$. An estimate of T_m can be obtained by solving Eq. (17) in the low-T limit $\omega T_1>>1$. This assumption is valid for $T\lesssim 5$ K, and is thus only applicable to the potassium (K) containing β-aluminas in Fig. 5. For $\omega T_1>>1$ Eq. (17) reduces to

$$\Delta\epsilon_{\rm rel}=\frac{2^{10}}{15}\frac{\pi}{\omega^2}\bar{P}p^2(kT)^6A^2\int_0^\infty dx\,x^6\cosh^2x\,. \tag{19}$$

The integral is equal to $\pi^6/42$. The minimum T_m is found from $(d/dT)(\Delta\epsilon_{\rm rel}+\Delta\epsilon_{\rm res})=0$. Assuming for simplicity that $(\bar{P}p^2)_{\rm rel}=(\bar{P}p^2)_{\rm res}$, we find

$$T_m^6=\frac{105}{128}\frac{\omega^2}{\pi^6}\frac{1}{A^2k^6}\,. \tag{20}$$

Given the experimental values of $T_m=3.2$ for Kβ-alumina and $T_m=4.0$ for $Na_{0.2}K_{0.8}$ β-alumina, we obtain from Eq. (20) that $A(\mathrm{K})=6.4\times10^7$ $\mathrm{sec}^{-1}\,\mathrm{K}^{-3}$ and $A(Na_{0.2}K_{0.8})=3.3\times10^7$ $\mathrm{sec}^{-1}\,\mathrm{K}^{-3}$. Using the experimentally determined relation of $(\bar{P}p^2)_{\rm rel}=2.7(\bar{P}p^2)_{\rm res}$ we find that $A(\mathrm{K})=3.9\times10^7$ $\mathrm{sec}^{-1}\,\mathrm{K}^{-3}$ and $A(Na_{0.2}K_{0.8})=2.0\times10^7$ $\mathrm{sec}^{-1}\,\mathrm{K}^{-3}$. These should be compared to the value for Naβ-alumina $A(\mathrm{Na})\cong2.5\times10^6$ $\mathrm{sec}^{-1}\,\mathrm{K}^{-3}$ which was obtained from conductivity data. The values for A can be expressed in terms of the coupling coefficient $\gamma=\gamma_l=\sqrt{2}\gamma_t$ in Eq. (10) as

$$\gamma^2=\frac{2\pi\rho\hbar^4}{1/v_l5+1/v_t5}A\,. \tag{21}$$

Given values of v_l, v_t and ρ for Na and Kβ-alumina from Table I we determine that $\gamma(\mathrm{Na})=0.3$ eV and $\gamma(\mathrm{K})=1.7$ eV for $A=6.4\times10^7$ $\mathrm{sec}^{-1}\,\mathrm{K}^{-3}$. If Eq. (20) is empirically corrected for $(\bar{P}p^2)_{\rm rel}\cong2.7(\bar{P}p^2)_{\rm res}$ then $\gamma(\mathrm{K})=1.4$ eV. Assuming the same values of ρ, v_l, v_t for $Na_{0.2}K_{0.8}$ that were used for Kβ-alumina we find $\gamma(Na_{0.2}K_{0.8})\cong0.72$ eV. The results for Na and Kβ-alumina compare favorably with those determined from low-frequency susceptibility[13] which are, respectively, $\gamma(\mathrm{Na})\cong0.3$ eV, $\gamma(\mathrm{K})\cong0.9$ eV.

The resonant contribution $\Delta\epsilon_{\rm res}\sim\bar{P}p^2\ln T/T_0$ provides a direct comparison of $\bar{P}p^2$ between the three β-aluminas. From Fig. 5 we obtain that

$$(\bar{P}p^2)_{\rm Na}\cong90(\bar{P}p^2)_{Na_{0.2}K_{0.8}}$$

and

$$(\bar{P}p^2)_{\rm Na}\cong250(\bar{P}p^2)_{\rm K}\,.$$

From specific-heat measurements below $T\sim1$ K, $\bar{P}(\mathrm{Na})\sim2.5\,\bar{P}(\mathrm{K})$,[10] which implies that the dipole moment for Naβ-alumina $p(\mathrm{Na})\sim10p(\mathrm{K})$. This result is at variance with susceptibility data at 10^2-10^4 Hz,[13] where $p(\mathrm{Na})\sim3.3p(\mathrm{K})$. It is possible that this discrepancy will be removed by including the ω^n contribution (to be discussed in Sec. III E) in the analysis of the 10^2-10^4 Hz suscepti-

TABLE I. Physical parameters for β-alumina. Note: v_t, v_l from Ref. 26; ϵ from Ref. 3; ρ from Ref. 10; and γ, $(\bar{P}p^2)_{\text{res}}$ from present work.

	Na	K
ρ (g cm^{-3})	3.22	3.33
v_t (cm sec^{-1})	3.8×10^5	4.3×10^5
v_l (cm sec^{-1})	9.1×10^5	9.5×10^5
ϵ	11.9	11.0
γ (eV)	0.3	1.4
$(\bar{P}p^2)_{\text{res}}$	1.7×10^{-3}	7×10^{-6}

bility data.

These results confirm the consequences which can be predicted qualitatively when substituting the larger K cation for Na ions. With increasing cation radius the cation sublattice becomes more rigid. This leads to a greatly reduced number of nearly equivalent cation sites and therefore reduced numbers of tunneling modes. The dipole moments associated with the tunneling modes are substantially reduced. Furthermore, the coupling of the cations to their environment, as evidenced by the magnitude of the deformation potential, is significantly increased. Such conclusions are quite in agreement with the observed increased local structural order as evidenced by an increasing correlation length in diffuse x-ray scattering for the cation sequence (Na,K,Rb)$-\beta$-alumina.[27]

The condition $\omega T_1 >> 1$ is not satisfied at temperatures $\gtrsim 10$ K which correspond to the minimum in $\Delta\epsilon$ for Naβ-alumina. For this case Eq. (17) needs to be solved numerically. A numerical fit with $A = 2.5\times10^6$ cm^{-1} K^{-3} in Eq. (17) to the $\Delta\epsilon$ data is unsatisfactory particularly at $T > 10$ K. Larger values for A and $(\bar{P}p^2)_{\text{rel}}$ result in a somewhat improved but still unsatisfactory fit. The discrepancies between theory and experiment for $\Delta\epsilon$ for Naβ-alumina are in part due to the contribution of the T^β term which has not been considered in Eq. (17), but which was taken into account in the fit to σ_{rel} (Fig. 5). The remaining difference between theory and experiment may be due to the contribution of the one-phonon Raman process which contributes an additional relaxation rate term to the direct one-phonon rate in Eq. (9). We have not attempted a precise fit to the dielectric constant data because of the uncertainty in the magnitude of the additional relaxation process. But as shown in the Appendix, the one-phonon Raman process could make contributions at those temperatures where significant differences are found between theory and experiment.

E. ac conductivity (10^2-10^4 Hz)

The temperature dependence of the ac conductivity of β-alumina for a wide frequency range is shown in Fig. 6.. The data at 10^2-10^4 Hz for $T < 10$ K are due to Anthony and Anderson.[13]

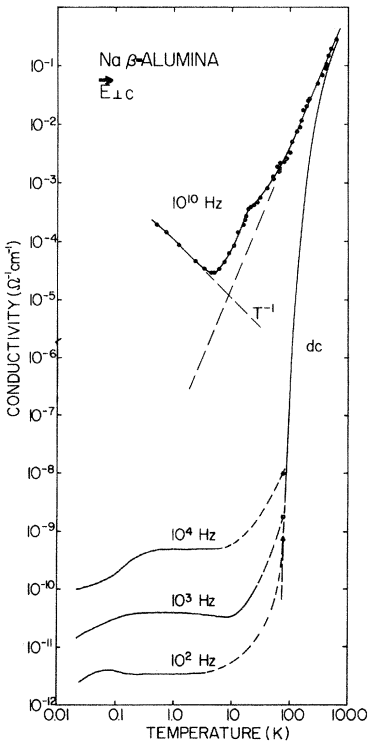

FIG. 6. Conduction plane conductivity of Naβ-alumina. 10 GHz data from Refs. 8 and 12. Data at 10^2-10^4 Hz: solid lines from Ref. 11; symbols from Ref. 28.

The three data points at these same frequencies but at higher temperatures, are from Grant *et al.*[28] No previous fit had been attempted to the low-frequency conductivity data, although Anthony and Anderson did fit the tunneling model to the dielectric constant data in the same frequency range.[13] We propose that the measured ac conductivity at 10^2-10^4 Hz between 0.1 and 10 K is dominated by tunneling modes. Results of a fit of $\sigma_{\rm rel}$ to the data are shown in Fig. 7. The solid lines represent the data.[13] The dotted lines represent $\sigma_{\rm rel}$ [as in Eq. (12)] with the *same* parameters, $(\bar{P}p^2)_{\rm rel}=4.3\times10^{-3}$ and $A=2.5\times10^6$ sec^{-1}K^{-3}, that were used to fit the microwave relaxation data. There is no significant contribution of resonant excitation of TLS at at 10^2-10^4 Hz for $T>0.1$ K, since $\sigma_{\rm res}\sim\omega^2$ for $kT>>\hbar\omega$, whereas the strongest frequency dependence for the relaxation contribution is $\sigma_{\rm rel}\sim\omega$ [Eq. (14)]. The correspondence of the step increase in the data with the rise to the relaxation plateau of $\sigma_{\rm rel}$ is evident in Fig. 7. Noteworthy also is the good agreement of the predicted and observed magnitudes of the ac conductivity with no adjustment of the microwave parameters.

In terms of the tunneling model, the nearly temperature-independent region observed between ~0.3 and 5 K at 10^2-10^4 Hz is a direct consequence of the broad distribution of relaxation times T_1.[13] If such a distribution did not exist, i.e., if we assumed only $T_1=T_{\rm min}$, then $\sigma_{\rm rel}$ would correspond to a single relaxation peak, which would fall off rapidly with increasing temperature $T\gtrsim1$ K, contrary to observation. These data,

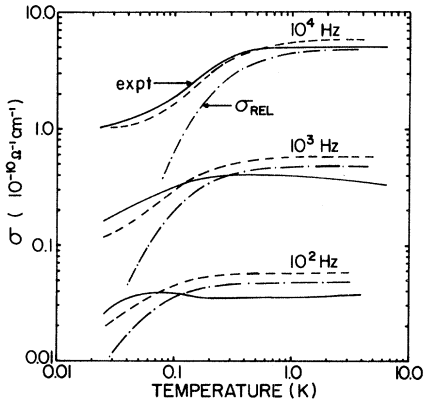

FIG. 7. ac conductivity of Naβ-alumina. Solid lines: data (Ref. 11); dashed dotted lines: $\sigma_{\rm rel}$ [Eq. (13)]; dashed lines: $\sigma_{\rm rel}+\sigma(0)\omega/\omega_0$ (parameters defined in text).

therefore, provide clear evidence for the existence of a broad distribution of relaxation times of tunneling modes.[29] At $T=0.5$ K this distribution ranges from $T_{\rm min}\simeq10^{-7}$ sec for modes with $E\sim kT$ to $T_{\rm max}>10^5\,T_{\rm min}$. A necessary consequence of the T distribution is the requirement that the low-temperature specific heat is time dependent. Recent observations suggest that this is indeed the case for glasses.[30] Comparable measurements on β-alumina should confirm these observations.

The additional conductivity for $T<0.1$ K cannot be accounted for by $\sigma_{\rm rel}$. The dashed line in Fig. 7 is an empirical fit with the total conductivity $\sigma(\omega,T)$ given by

$$\sigma(\omega,T)=\sigma_{\rm rel}(\omega,T)+\sigma(0)(\omega/\omega_0)^n\,, \tag{22}$$

where $n\simeq1.0$, $\sigma(0)=1.0\times10^{-10}\,\Omega^{-1}$ cm^{-1}, and $\omega_0/2\pi=10^4$ sec^{-1}. The first term is identical to the dotted-dashed lines in Fig. 7. The second term, which is temperature independent, is reminiscent of the well known $\sigma\sim\omega^n$ ($n\lesssim1$) conductivity observed in many disordered solids for $\omega/2\pi<10^8$ sec^{-1} (Ref. 31). Depending on specific model assumptions such a conductivity is generally predicted to saturate in magnitude at frequencies above 10^8 Hz. This is required for Naβ-alumina since there is no evidence for a temperature-independent contribution to σ at $\omega/2\pi\sim10^{10}$ sec^{-1}. A frequency saturation of the $\sim T^2$-dependent conductivity observed for $T>50$ K in the 10^9-10^{11}-Hz range has already been reported.[8] We suggest that there is a close relationship between the temperature-independent ac conductivity observed at temperature below 0.1 K and the $\sim BT^\beta$ high-temperature conductivity for $T>50$ K. A preliminary discussion of this point has been presented recently.[32]

F. Structural origin of tunneling modes

The physical origin of tunneling modes in glassy solids is still unknown. Specific suggestions for various types of disordered materials have been made; however, these are generally difficult to verify. By contrast, structural-tunneling modes in crystalline solids are well defined. For example, protons in ferroelectric KDP (potassium dihydrogen phosphate) have the possibility of occupying two nearly equivalent sites separated by a potential barrier. With insufficient thermal energy, the pro-

tons will quantum-mechanically tunnel through the barrier. The situation in β-alumina is analogous in the sense that an ion can tunnel through a potential barrier between two nearly equivalent configurations. The complexity arises from the lack of knowledge of how large the tunneling unit is (i.e., single ion versus groups of ions) and what interaction leads to the extensive broadening of the density of states of tunneling energies. However, since a subset of the tunneling-level splittings is probed with the resonant absorption of microwave radiation, some predictions of tunnel-mode parameters can be made.

From Eqs. (2) and (4) we find for symmetric wells ($\Delta=0$) that $E=\Delta_0=\hbar\Omega e^{-\lambda}$ where $\lambda=d(2mV/\hbar^2)^{1/2}$. For $E=\hbar\omega$, $e^{-\lambda}=\omega/\Omega$. Reasonable values of Ω (a phonon energy) range from 10^{10} to 10^{13} Hz, i.e., $\lambda\simeq 1-10$. The *smallest* tunneling unit is a single Na^+. For $m=m_{Na^+}$ and $d=1$ Å, $V=2.5$ meV, which is a small barrier height compared to the dc activation energy of 0.16 eV.

Possible single-particle tunneling modes can be identified when examining the conducting plane of β-alumina in Fig. 8. For example, whenever 2 MO sites are occupied by Na^+, then for 50% of such cases the third MO site is unoccupied (otherwise, it is occupied by a charge compensating O^{2-} ion). As was already pointed out by McWhan *et al.*,[9] the ion may tunnel from one MO site to another. Because of different local Coulombic fields at each such a tunneling mode due to differences in the local environments (i.e., other Na^+, O^{2-} etc.), the distribution function $n(E)$ will be broad compared to the absolute magnitude of E. Microscopic calculations are necessary in order to verify if local barrier heights between equivalent MO sites are of the required magnitude ($\sim$meV). In addition, the movement of larger groups of ions needs to be considered.

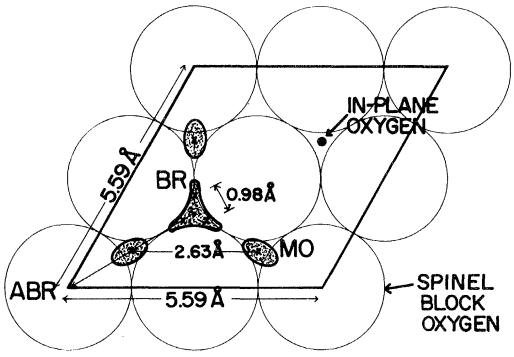

FIG. 8. Conduction plane of Naβ-alumina. BR: Beevers-Ross site; MO: mid-oxygen site; ABR: anti-Beevers-Ross site (from Ref. 7).

A recent theoretical study by Cohen and Grest[33] on the possible origin of tunneling modes in glasses suggests a close relationship between structural changes near the glass transition temperature T_g and the formation of tunneling modes which are observable at low temperatures. According to this view, liquid clusters are frozen in as the glass has its temperature lowered through T_g. At yet lower temperatures, the trapped liquid regions themselves freeze, leading to the formation of voids within them. It is suggested that the movement of atoms into these voids constitutes the tunneling centers. Phillips[34] has proposed a related interpretation with specific emphasis on chalcogenide glasses but with possibly more general applicability. In Phillips's view microvoids are highly crosslinked, leading to well-defined clusters. Certain crosslinking atoms are identified as two-level tunneling centers. These models may have some validity for β-alumina.

The system of mobile cations in the conduction-plane structure resembles a "glass" at low temperatures. It has been recently suggested[32] that as the temperature is raised this system undergoes a "glass transition" in the range of $T\sim 100$ K. Above this temperature the glasslike states will dissociate into mobile cations. There is some corroborating evidence for a "glass transition" in Naβ-alumina near $T_g\sim 100$ K from specific-heat and nuclear-magnetic-resonance (NMR) measurements.[35] In particular, the NMR results point toward formation of domain-like regions below $T\sim 100$ K. Application of the theoretical arguments by Cohen and Grest and Phillips to Naβ-alumina suggest that microdomain formation could result in local two-dimensional voids of irregular size and shape. Crosslinking could result in cluster or domain formation as evidenced by NMR measurements. Such clusters may be related to the "associated regions" discussed by Wolf[36] for β-alumina which contain two or more MO-paired cations formations with associated charge-compensating in-plane oxygen ions. Even though tunneling modes may be formed by nearly equivalent MO sites in the interior of a cluster, it is possible that TLS may be associated with the "surface ions" of the associated regions.

IV. CONCLUSION

The standard tunneling model of two-level systems has been applied to describe the low-temperature microwave dielectric properties of Naβ-alumina. Contributions to the dielectric loss due to resonant and relaxation absorption could be identified. The TLS model provides an accurate description of the resonant contribution, but somewhat underestimates the relaxation contribution if only direct one-phonon processes are considered. The possible involvement of a one-phonon Raman process has been outlined. The importance of TLS relaxation contributions to the ac conductivity at 10^2-10^4 Hz has been stressed. A direct relationship between the microwave relaxation region and portions of the 10^2-10^4-Hz data can be established. It was shown that 10^2-10^4-Hz data additionally require the existence of a temperature-independent conductivity term $\sigma\sim\omega^n$ where $n\cong 1$ for $T<1$ K. This contribution saturates in magnitude above $\sim 10^8$ Hz. The possible close relationship between the ω^n conductivity and the temperature-dependent term BT^β where $\beta\cong 2$ has been discussed. Details of this relationship as well as the study of microwave dielectric echoes at ultra-low temperatures in Naβ-alumina will be treated in separate publications.

ACKNOWLEDGMENTS

Helpful discussions with B. Golding, A. C. Anderson, and T. L. Reinecke are gratefully acknowledged.

APPENDIX

The relaxation of TLS by a one-phonon Raman process will be considered here. The relaxation rate for the direct one-phonon process is given by Eq. (9) (letting $T_1\equiv\tau_D$) as

$$\tau_D^{-1}=A\left[\frac{\Delta_0}{E}\right]^2 E^3\coth(E/2kT)\ , \tag{A1}$$

where A is defined by Eq. (10). The one-phonon Raman relaxation rate is given by

$$\tau_R^{-1}=B\left[\frac{\Delta_0}{E}\right]^2 (T)^7\ , \tag{A2}$$

with

$$B=\frac{9\gamma_R^2 k^3}{2\pi^2\rho^2 v_t^{10}}\frac{J_R}{\hbar^7}\ , \tag{A3}$$

where γ_R is a coupling parameter and

$$J_R=(1-e^{E/kT})\int_0^{\hbar\omega_D/kT}\frac{x^3e^x dx}{(e^x-1)(e^{x-E/kT}+1)}\ . \tag{A4}$$

The main contribution to J_R comes from those states for which $E\sim kT$. For $\hbar\omega_D>>kT$ then J_R is only weakly temperature dependent. We introduce the following abbreviations:

$$\tau^{-1}=\tau_D^{-1}+\tau_R^{-1}=\left[\frac{\Delta_0}{E}\right]^2\tau_{\min}^{-1}\ , \tag{A5}$$

i.e.,

$$\tau^{-1}=\left[\frac{\Delta_0}{E}\right]^2\left[AE^3\coth\frac{E}{2kT}+BT^7\right]\ . \tag{A6}$$

We also define $M=\omega\tau_{\min}$, $x=E/kT$, $u=\Delta/E$, and $\omega\tau=M/(1-u^2)$. The absorption $\alpha_{\rm rel}$ then becomes, according to Eq. (13):

$$\alpha_{\rm rel}=\frac{16\pi\bar{P}p^2}{c\sqrt{\epsilon}}\omega\int_0^\infty dx\,\frac{e^x}{(1+e^x)^2}\int_0^1\frac{duMu^2}{(1-u^2)^2+M^2}\ . \tag{A7}$$

The second integral can be solved directly:

$$\begin{aligned}J_\alpha&=\int_0^1\frac{duMu^2}{(1-u^2)^2+M^2}\\&=\frac{M\sqrt{N+1}-\sqrt{N-1}}{2\sqrt{2N}}\ln\frac{M}{N+1-\sqrt{2}(N+1)}\\&\quad-\frac{\sqrt{N+1}+M\sqrt{N-1}}{2\sqrt{2N}}\tan^{-1}\frac{\sqrt{2}}{\sqrt{N-1}}\ ,\end{aligned} \tag{A8}$$

where $N=\sqrt{1+M^2}$.

Consider the following limits: (a) For $M\to 0$; i.e., $\omega\tau_{\min}<<1$ ("high"-temperature case), we find that $J_\alpha\to-\pi/4$. Solving the first integral in Eq. (A7) directly yields

$$\alpha_{\rm rel}=\frac{2\pi^2\bar{P}p^2\omega}{c\sqrt{\epsilon}}\ , \tag{A9}$$

which is *independent* of the nature of the relaxation process. (b) For $M\to\infty$; i.e., $\omega\tau_{\min}>>1$ ("low"-temperature case), $J_\alpha\to-1/3M$ and Eq. (A7) becomes

$$\alpha_{\rm rel}=\frac{\pi\bar{P}p^2}{3c\sqrt{\epsilon}}(\pi^4Ak^3T^3+8BT^7)\ . \tag{A10}$$

Depending on the relative sizes of A and B, it is possible that the second term will contribute significantly to the absorption in an intermediate temperature range and may thus account for the somewhat steeper slope of the conductivity observed in Naβ-alumina at 11.5 GHz between 5 and 25 K.

The variation of the dielectric constant has the form

$$\Delta\epsilon = 16\pi\bar{P}p^2 \int_0^\infty dx \frac{e^x}{(1+e^x)^2} \int_0^1 \frac{u^2(1-u^2)du}{(1-u^2)^2+M^2} , \tag{A11}$$

where

$$\int_0^1 \frac{u^2(1-u^2)du}{(1-u^2)^2+m^2} \equiv J_\epsilon = \frac{\sqrt{N+1}+M\sqrt{N-1}}{2\sqrt{2}N} \ln \frac{M}{N+1-\sqrt{2(N+1)}} - \frac{\sqrt{N-1}-M\sqrt{N+1}}{2\sqrt{2}N} \tan^{-1} \frac{\sqrt{2}}{\sqrt{N-1}} - 1 . \tag{A12}$$

The limiting cases are (a) $M \to 0$; i.e., $\omega\tau_{\min} << 1$, then

$$J_\epsilon \to \tfrac{1}{2} \ln \frac{4}{M} - 1$$

and

$$\Delta\epsilon = 16\pi\bar{P}p^2 \int dx \frac{e^x}{(1+e^x)^2} \left[\frac{1}{2} \ln \frac{4}{M} - 1 \right] . \tag{A13}$$

It is easily shown that $\Delta\epsilon$ for the direct one-phonon process is given by

$$\Delta\epsilon_D = 4\pi\bar{P}p^2 \left[\left[\ln \frac{T^3}{\omega} + \ln 4Ak^3 - 2 \right] + 2\int_0^\infty \frac{e^x}{(1+e^x)^2} \ln x^3 \coth \frac{x}{2} dx \right] .$$

Hence,

$$\Delta\epsilon_D = 4\pi\bar{P}p^2(\text{const} + 3\ln T/\omega) . \tag{A14}$$

For the one-phonon Raman process we find

$$\Delta\epsilon_R = 4\pi\bar{P}p^2(\text{const} + 7\ln T/\omega) . \tag{A15}$$

Comparison of Eq. (A14) with Eq. (A15) shows that $\Delta\epsilon$ is enhanced by the Raman process by a factor of $\frac{7}{3}$. In case (b), $M \to \infty$ ($\omega\tau_{\min} >> 1$). In this limit J_ϵ becomes

$$J_\epsilon \to \frac{2}{15} \frac{1}{M^2} . \tag{A16}$$

For the direct one-phonon process $M \sim \omega/(AE^3 \coth x/2)$ so that

$$\Delta\epsilon_D \sim A^2T^6 . \tag{A17}$$

For the Raman process, $M \sim \omega/BT^7$, so that

$$\Delta\epsilon_R \sim B^2T^{14} . \tag{A18}$$

At sufficiently low T, the Raman process is unlikely to compete with the direct process. However, $\Delta\epsilon_R$ may make a significant contribution at higher T. Note that in both high- and low-temperature limits there is an enhancement in $\Delta\epsilon$ due to the one-phonon Raman process, whereas the high-temperature limit of α [Eq. (A9)] is independent of the details of the process.

[1] S. J. Allen, Jr. and J. P. Remeika, Phys. Rev. Lett. 33, 1478 (1974).

[2] P. B. Klein, D. E. Schafer, and U. Strom, Phys. Rev. B 18, 4411 (1978).

[3] S. J. Allen, Jr., A. S. Cooper, F. DeRosa, J. P. Remeika, and S. K. Ulasi, Phys. Rev. B 17, 4031 (1978).

[4] C. H. Hao, L. L. Chase, and G. D. Mahan, Phys. Rev. B 13, 4306 (1976).

[5] J. C. Wang, M. Gaffari, and Sang-il Choi, J. Chem. Phys. 63, 772 (1975).

[6] M. S. Whittingham and R. Huggins, J. Chem. Phys. 54, 414 (1971).

[7] C. Peters, M. Bettman, J. Moore, and M. Glock, Acta Crystallogr. Sect. B 27, 1826 (1971).

[8] U. Strom, P. C. Taylor, S. G. Bishop, T. L. Reinecke, and K. L. Ngai, Phys. Rev. B 13, 3329 (1976).

[9]D. B. McWhan, C. M. Varma, F. L. S. Hsu, and J. P. Remeika, Phys. Rev. B 15, 553 (1977).
[10]P. J. Anthony and A. C. Anderson, Phys. Rev. B 16, 3827 (1977).
[11]P. J. Anthony and A. C. Anderson, Phys. Rev. B 14, 5198 (1976).
[12]U. Strom, M. von Schickfus, and S. Hunklinger, Phys. Rev. Lett. 41, 910 (1978).
[13]P. J. Anthony and A. C. Anderson, Phys. Rev. B 19, 5310 (1979).
[14]Preliminary account of electric-field echo experiments in Naβ-alumina has been given by M. von Schickfus and U. Strom, Bull. Am. Phys. Soc. 25, 196 (1980).
[15]U. Strom and P. C. Taylor, J. Appl. Phys. 50, 5761 (1979).
[16]G. Birnbaum and J. Franeau, J. Appl. Phys. 20, 817 (1949).
[17]M. von Schickfus and S. Hunklinger, Phys. Lett. A 64, 144 (1977); M. von Schickfus, Ph.D. dissertation, Technische Universität München, 1975 (unpublished).
[18]R. E. Walstedt, R. Dupree, J. P. Remeika, and A. Rodriguez, Phys. Rev. B 15, 3442 (1977).
[19]J. Jäckle, Z. Phys. 257, 212 (1972).
[20]S. Hunklinger and W. Arnold, in *Physical Acoustics*, edited by W. P. Mason and R. N. Thurston (Academic, New York, 1976), Vol. 12, p. 155.
[21]J. E. Graebner and B. Golding, Phys. Rev. B 19, 964 (1979).
[22]J. L. Black and B. I. Halperin, Phys. Rev. B 16, 2879 (1977).
[23]J. L. Black, Phys. Rev. B 17, 2740 (1978).
[24]B. Golding, J. E. Graebner, A. B. Kane, and J. L. Black, Phys. Rev. Lett. 41, 1487 (1978).
[25]B. Golding, M. von Schickfus, S. Hunklinger, and K. Dransfeld, Phys. Rev. Lett. 43, 1817 (1979).
[26]D. B. McWhan, S. M. Shapiro, J. P. Remeika, and G. Shirane, J. Phys. C 8, L487 (1975).
[27]D. B. McWhan, S. S. Allen, Jr., J. P. Remeika, and P. D. Dernier, Phys. Rev. Lett. 35, 953 (1975); 36, 344 (E) (1976).
[28]R. J. Grant, I. M. Hodge, M. D. Ingram, and A. R. West, Nature 266, 42 (1977).
[29]Comparable evidence is provided by the recent ultrasonic measurements of T. Doussineau, C. Frénois, R. G. Leisure, A. Levelut, and J. Y. Rieur, J. Phys. (Paris) 41, 1193 (1980).
[30]M. T. Loponen, R. C. Dynes, V. Narayanamurti, and J. P. Garno, Phys. Rev. Lett. 45, 457 (1980).
[31]A. K. Jonscher, F. Meca, and H. M. Millany, J. Phys. C 12, L293 (1979).
[32]U. Strom and K. L. Ngai, Solid State Ion. 5, 167 (1981).
[33]M. H. Cohen and G. S. Grest, Phys. Rev. Lett. 45, 1271 (1980).
[34]J. C. Phillips (private communication).
[35]J. L. Bjorkstam, P. Ferloni, and M. Villa, J. Chem. Phys. 73, 2932 (1980).
[36]D. J. Wolf, J. Phys. Chem. Solids 40, 757 (1979).